

Oxidative Addition of Carbon-Carbon Bonds with a Redox-Active Bis(imino)pyridine Iron Complex.

Jonathan M. Darmon,^{a,d} S. Chantal E. Stieber,^d Kevin T. Sylvester,^a Ignacio Fernández,^b Emil Lobkovsky,^a Scott P. Semproni,^d Eckhard Bill,^c Karl Wieghardt,^{*c} Serena DeBeer,^{*a,c} and Paul J. Chirik^{*d}

^a *Department of Chemistry and Chemical Biology, Baker Laboratory, Cornell University, Ithaca, New York, U. S. A. 14850*

^b *Área de Química Orgánica, Universidad de Almería, Carretera de Sacramento s/n Almería, Spain*

^c *Max-Planck Institute for Chemical Energy Conversion, Stiftstrasse 34-36, D-45470 Mülheim an der Ruhr, Germany*

^d *Department of Chemistry, Princeton University, Princeton, New Jersey, U. S. A. 08544*

pchirik@princeton.edu

Supporting Information

Table of Contents

Experimental Procedures	S3
A. General Considerations	S3
B. Additional Compound Preparations	S5
Variable Temperature ^1H NMR Spectra	S7
SQUID Data for (^iPr PDI)Fe(biphenylene)	S9
Variable Temperature ^{57}Fe Mössbauer Data	S12
Additional Magnetic and Spectroscopic Data	S13
Computational Results	S16
References	S21

Experimental Section

A. General Considerations.

All air- and moisture-sensitive manipulations were carried out using standard vacuum line, Schlenk and cannula techniques or in an MBraun inert atmosphere drybox containing an atmosphere of purified nitrogen. The MBraun drybox was equipped with a cold well designed for freezing samples in liquid nitrogen. Solvents for air- and moisture-sensitive manipulations were initially dried and deoxygenated using literature procedures.¹ Argon and dihydrogen gas were purchased from Airgas Incorporated and passed through a column containing manganese oxide supported on vermiculite and 4 Å molecular sieves before admission to the high vacuum line. Benzene-*d*₆ was purchased from Cambridge Isotope Laboratories and distilled from sodium metal under an atmosphere of argon and stored over 4 Å molecular sieves or sodium metal. CDCl₃ was purchased from Cambridge Isotope Laboratories and used as received or distilled from calcium hydride. The bis(imino)pyridine iron dinitrogen compounds, (ⁱPrPDI)Fe(N₂)₂² and [(^{Me}PDI)Fe(N₂)]₂(μ₂-N₂),³ were prepared according to literature procedures.

¹H NMR spectra were recorded on Varian Mercury 300, Inova 400 and 500 spectrometers operating at 299.763, 399.780 and 500.62 MHz, respectively. All chemical shifts are reported relative to SiMe₄ using ¹H (residual) chemical shifts of the solvent as a secondary standard. For paramagnetic molecules, the ¹H NMR data are reported with the chemical shift followed by the peak width at half height in Hertz or multiplicity, followed by integration value and where possible, peak assignment.

Single crystals suitable for X-ray diffraction were coated with polyisobutylene oil in a drybox, transferred to a nylon loop and then quickly transferred to the goniometer head of a Bruker APEX2 ((ⁱPrPDI)Fe(biphenyl)) or Bruker X8 APEX2 Duo ((^{Me}PDI)Fe(biphenyl)) diffractometer equipped with a molybdenum X-ray tube ($\lambda = 0.71073 \text{ \AA}$). Preliminary data

revealed the crystal system. Data collection routines were optimized for completeness and redundancy using the Bruker COSMO software suite. The space group was identified, and the data were processed using the Bruker SAINT+ program and corrected for absorption using SADABS. The structures were solved using direct methods (SHELXS) completed by subsequent Fourier synthesis and refined by full-matrix least-squares procedures.

Mass spectra were acquired using a JEOL GCMate II mass spectrometer operating at 500 (LRMS) or 3000 (HRMS) resolving power (20% FWHM) in positive ion mode and an electron ionization (EI) potential of 70 eV. Samples were introduced via a GC inlet using an Agilent HP 6890N GC equipped with a 30 m (0.25 μ i.d.) HP-5ms capillary GC column. The carrier gas is helium with a flow rate of 1 mL/min. Samples were introduced into the GC using a split/splitless injector at 230 °C with a split ratio of 10:1 (HRMS) or 50:1 (LRMS).

Solution magnetic moments were determined by the method of Evans⁴ using a ferrocene standard and are the average value of two to three independent measurements. Solid state magnetic susceptibility measurements were performed with a Johnson Matthey magnetic susceptibility balance (MSB) that was calibrated with HgCo(SCN)₄ or using SQUID magnetometry. Variable temperature (4-300 K) magnetization data were recorded in a 1 T magnetic field on a MPMS Quantum Design SQUID magnetometer. The experimental magnetic susceptibility data were corrected for underlying diamagnetism using tabulated Pascal's constants.⁵ SQUID data were modeled using the programs JulX and PhaseT (by Eckhard Bill). Elemental analyses were performed at Robertson Microlit Laboratories, Inc. in Madison, NJ.

Zero-field ⁵⁷Fe Mössbauer spectra were recorded on a SEE Co. Mössbauer spectrometer (MS4) at 80 K in constant acceleration mode. ⁵⁷Co/Rh was used as the radiation source. WMOSS software was used for the quantitative evaluation of the

spectral parameters (least-squares fitting to Lorentzian peaks). The minimum experimental line widths were 0.23 mm/s. Good quality data has fit line widths that are less than 0.4 mm/s. The temperature of the sample was controlled by a Janis Research Co. CCS-850 He/N₂ cryostat within an accuracy of 0.3 K. Applied field Mössbauer data were collected using an Oxford Instruments Mössbauer-Spectromag cryostat, where the split-pair superconducting magnet system allows applied fields up to 8 T and the temperature of the samples can be varied in the range of 1.5-250 K. The field at the sample is perpendicular to the γ beam. Magnetic Mössbauer spectra were simulated with the program MX (by Eckhard Bill). Isomer shifts were determined relative to α -iron at 298 K.

XAS data were collected at the Stanford Synchrotron Radiation Lightsource (SSRL) on beamline 9-3 under standard ring conditions and measured and handled and fit (Simpson's Rule method) as previously described.⁶ Variable temperature experiments were conducted on two separate samples in which one was first measured at 10 K followed by warming to 298 K and the second sample was first measured at 298 K followed by cooling to 10 K. The data were overlaid to confirm that the low temperature data were identical, and that the high temperature data were identical. XES data were collected at the Cornell High Energy Synchrotron Source (CHESS) on beamline 6-2 for (ⁱPrPDI)Fe(biphenyl) using previously described conditions and methods.⁶ All geometry optimizations and spectroscopic calculations were performed as previously described using the ORCA program package (version 2.7.0).^{6,7}

B. Additional Preparation of Compounds.

Preparation of Biphenylene. Biphenyl (10.0 g, 64.9 mmol) was suspended in 25 mL of dry N, N, N', N'-tetramethylethylenediamine in a 250-mL round bottom flask under an atmosphere of argon. A solution of *n*-butyl lithium (100 mL, 1.4 M, 140 mmol) in hexanes

was added dropwise to the suspension and stirred for 3 days at room temperature. During this time the reaction turned from light yellow to dark red. After three days approximately 200 mL of pentane was added to the reaction mixture and it was filtered under argon. The solid was collected and dried to yield 14.8 g of a dark yellow powder (57.6 % yield) identified as the expected dilithio salt of biphenylene. This product (7.56 g, 19.0 mmol) and dry zinc dichloride (6.17 g, 45.4 mmol) were charged into a 250 mL round bottom flask. Approximately 25 mL of dry THF (125 mL) were added by vacuum transfer to the mixture at -78 °C. The reaction mixture was warmed to room temperature and stirred for three hour under argon. Dry copper (II) chloride (6.17 g, 45.8 mmol) was then added and the reaction was stirred again at -78 °C for two hours. Aqueous HCl (45 mL, 4 M) was added to the reaction mixture, which was then extracted with toluene (3 x, 80 mL). The combined organic layers were washed with water (2x, 50 mL), then brine (25 mL), and dried over sodium sulfate. The drying reagent was removed via filtration and the solvent was removed under reduced pressure to yield 1.45 g of a brown solid. The brown solid was recrystallized was hot cyclohexane to yield 0.940 g (33 %) of yellow needles identified as biphenylene. Spectral properties were consistent with previous reported results.⁸

Transfer Hydrogenation from (^RPDI)Fe(biphenyl). A solution of 0.010 g of (ⁱPrPDI)Fe(biphenyl) (0.015 mmol) in 0.50 mL of benzene-*d*₆ was prepared in a J. Young NMR tube. After standing at room temperature for 30 hours, a color change from green to brown was observed and all of the paramagnetic resonances attributed to the starting iron compound disappeared in the ¹H NMR spectrum. Degradation of the reaction mixture by addition of water resulted in the observation of one equivalent of free ligand (ⁱPrPDI) and one equivalent of biphenyl by ¹H NMR spectroscopy.

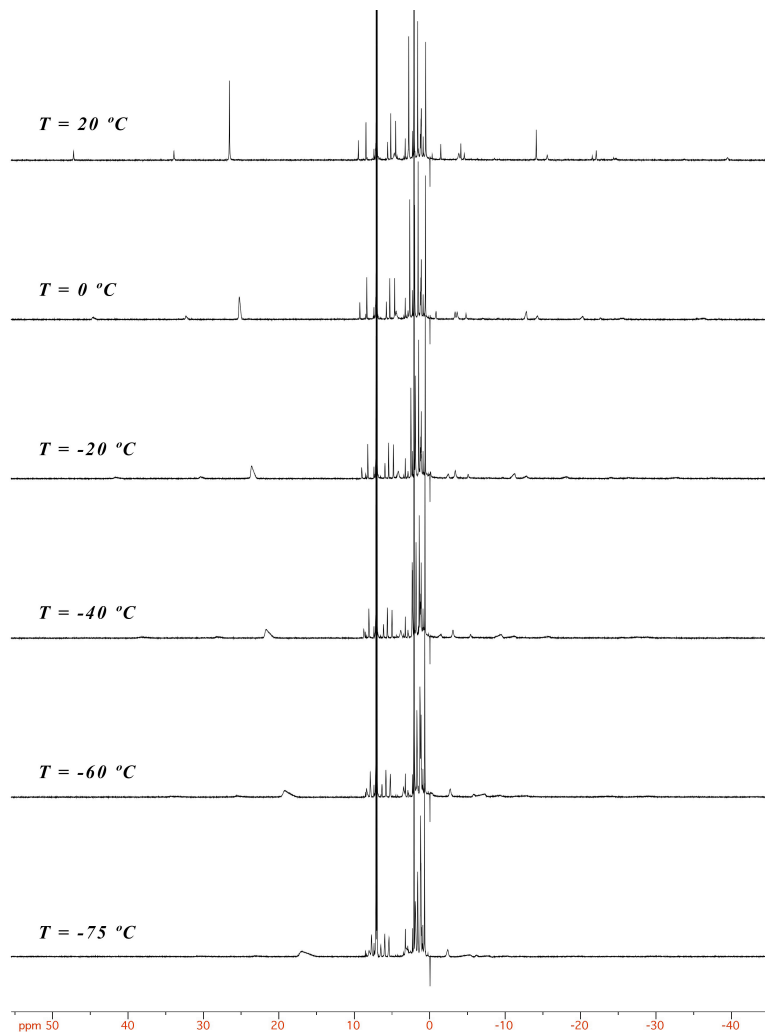


Figure S1. Variable temperature ^1H NMR spectra of $(i\text{PrPDI})\text{Fe}(\text{biphenyl})$ in $\text{toluene-}d_8$.

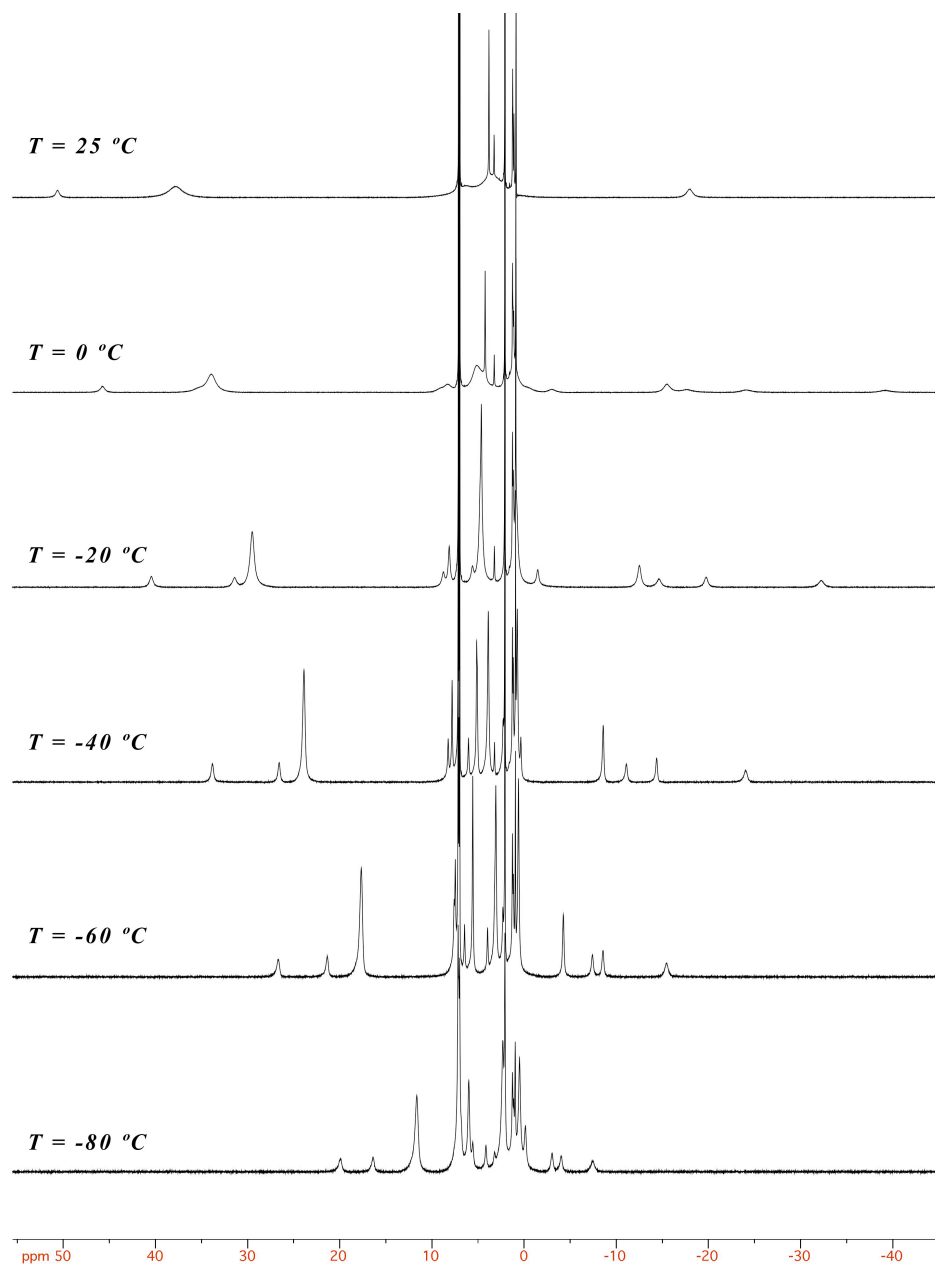


Figure S2. Variable temperature ^1H NMR spectra of $(^{\text{Me}}\text{PDI})\text{Fe}(\text{biphenyl})$ in $\text{toluene-}d_8$.

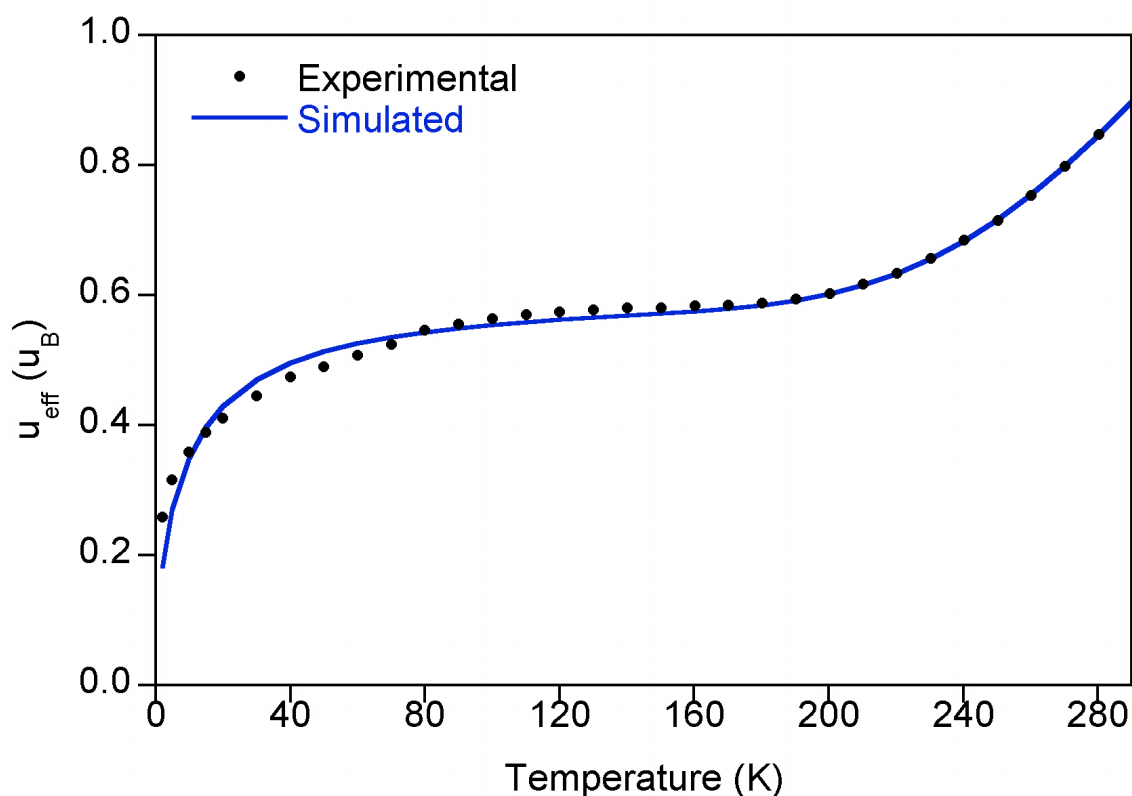


Figure S3. SQUID magnetic data (i^{Pr} PDI)Fe(biphenyl). Variable temperature SQUID magnetization data for (i^{Pr} PDI)Fe(biphenyl) from 4-300 K. Data (black dots) are corrected for underlying diamagnetism and the simulation (blue line) depicts a phase transition from an $S = 0$ to $S = 1$ state (as fit using the Sorai and Seki domain model)^{9,10} with a transition temperature of 511 K and enthalpy, $n\Delta H = 1298 \text{ cm}^{-1}$. The data was additionally modeled additionally with $\text{TIP} = 1700 \text{ cm}^{-1}$ and contains 1 % of a paramagnetic impurity with $\theta = -20 \text{ K}$. The high TIP and presence of the paramagnetic impurity are likely due to the instability of and difficulty in handling this compound. However, the rapid increase in effective magnetic moment above 200 K is indicative of spin crossover behavior and is not largely affected by these two parameters.

Table S1. Variable temperature zero-field ^{57}Fe Mössbauer parameters for ($^{i\text{Pr}}$ PDI)Fe(biphenyl).

Temperature	δ (mm/sec)	ΔE_Q (mm/s) ^a
10	0.07	3.67
80	0.07	3.66
150	0.05	3.63
200	0.04	3.59
250	0.01	3.51

^a All values of ΔE_Q are absolute values.

Table S2. Variable temperature zero-field ^{57}Fe Mössbauer parameters for ($^{\text{Me}}$ PDI)Fe(biphenyl).

Temperature	δ (mm/sec)	ΔE_Q (mm/s) ^a
10	0.07	3.77
80	0.06	3.76
295	-0.02	3.43

^a All values of ΔE_Q are absolute values.

Table S3. Experimental and computed bond lengths (Å) and angles (deg) for (ⁱPrPDI)Fe(biphenyl).

	Experimental	BS(3,1)	BS(1,1)	RKS
Fe(1)-N(1)	1.9402(18)	2.134	2.034	2.023
Fe(1)-N(2)	1.8569(16)	1.915	1.893	1.880
Fe(1)-N(3)	1.9503(18)	2.136	2.033	2.028
Fe(1)-C(26)	1.9436(19)	2.033	1.944	1.952
Fe(1)-C(37)	1.9656(19)	1.988	1.993	1.989
N(1)-C(2)	1.318(2)	1.314	1.315	1.306
N(3)-C(8)	1.320(2)	1.314	1.316	1.306
N(2)-C(3)	1.363(3)	1.369	1.365	1.356
N(2)-C(7)	1.366(2)	1.368	1.365	1.356
C(2)-C(3)	1.452(3)	1.455	1.457	1.465
C(7)-C(8)	1.447(3)	1.456	1.456	1.465
N(2)-Fe(1)-C(26)	92.47(7)	99.0	99.4	93.7
N(2)-Fe(1)-C(37)	175.93(8)	178.5	176.0	178.9

Table S4. Experimental and computed ⁵⁷Fe Mössbauer spectroscopic parameters and relative computed ground state energies for (^{Me}PDI)Fe(biphenyl).

	Experimental 80 K	Experimental 295 K	BS(3,1)	BS(1,1)	RKS
relative calculated energy (kcal)	NA	NA	0.0	+7.2	+13.1
δ (mm/s)	0.05	-0.02	0.16	0.06	0.11
ΔE _Q (mm/s)	3.69	3.43	+3.58	+2.72	+2.95
η	—	—	0.36	0.12	0.95

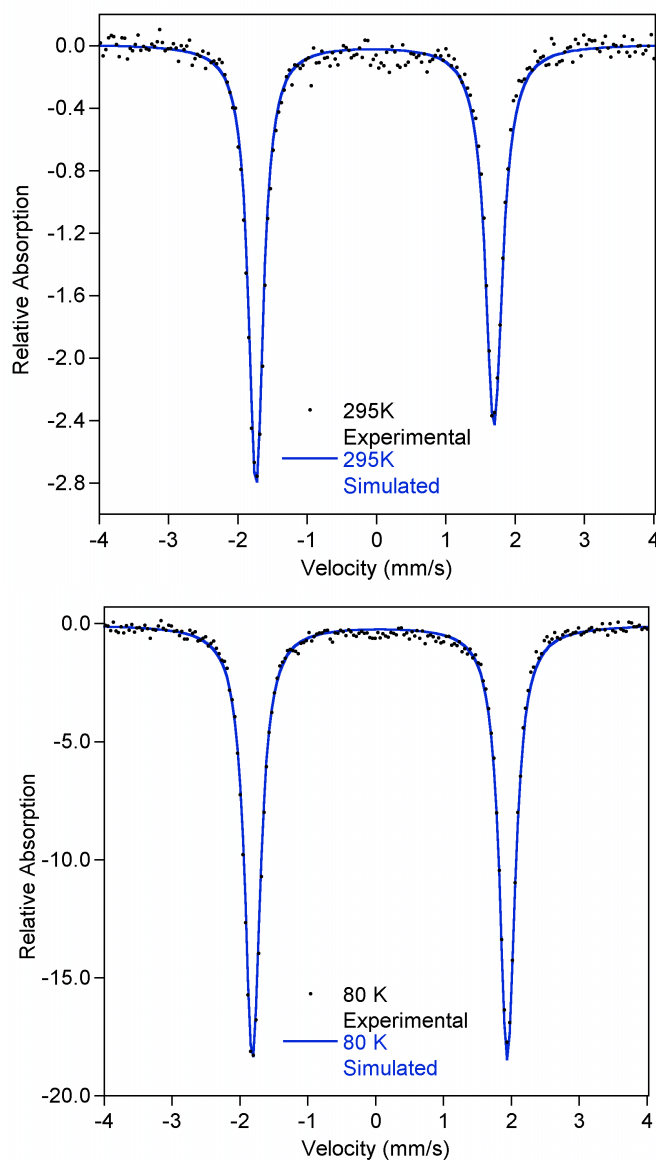


Figure S4. Zero-field ^{57}Fe Mössbauer spectra of $(^{\text{Me}}\text{PDI})\text{Fe}(\text{biphenyl})$ at 80 K (bottom) and 295 K (top). Simulated parameters (blue lines) are $\delta = 0.05$ mm/s, $\Delta E_{\text{Q}} = 3.69$ mm/s at 80 K and $\delta = -0.02$ mm/s, $\Delta E_{\text{Q}} = 3.43$ mm/s at 295 K.

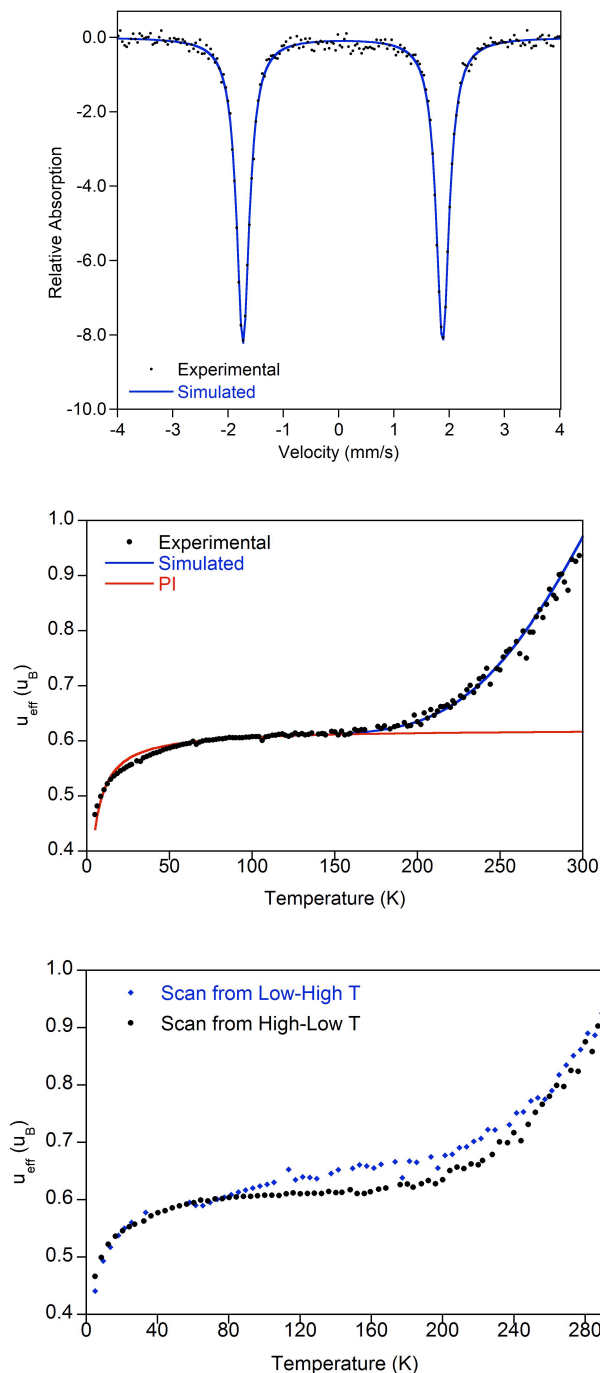


Figure S5. Zero-field ^{57}Fe Mössbauer spectrum (top) of $(i\text{PrPDI})\text{Fe}(\text{biphenyl})$ at 80 K on the same sample used for magnetic measurement (middle). Data (black dots) are corrected for underlying diamagnetism and TIP (720cm^{-1}) and the simulation (blue line) depicts a phase transition from an $S = 0$ to $S = 1$ state (as fit using the Sorai and Seki domain model)^{9,10} with a transition temperature of 511 K and enthalpy, $n\Delta H = 1298\text{ cm}^{-1}$. The model additionally contains 1.1 % of a paramagnetic impurity (red line) with $\theta = -5$ K. Temperature was scanned from 5-300 K (blue) and 300-5 K (black) to eliminate hysteresis (bottom). Data are corrected for underlying diamagnetism and TIP (720 cm^{-1}), and points which are statistical outliers are omitted.

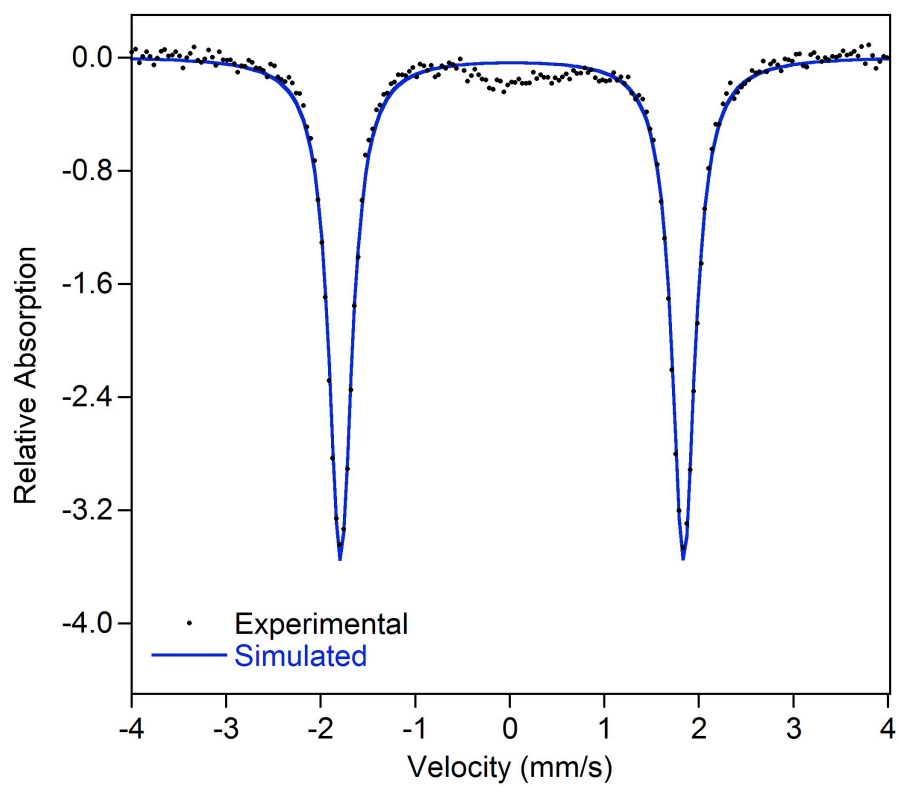


Figure S6. Zero-field ^{57}Fe Mössbauer spectrum of $(^{\text{Me}}\text{PDI})\text{Fe}(\text{biphenyl})$ recorded at 80 K on the same sample used for magnetic measurements.

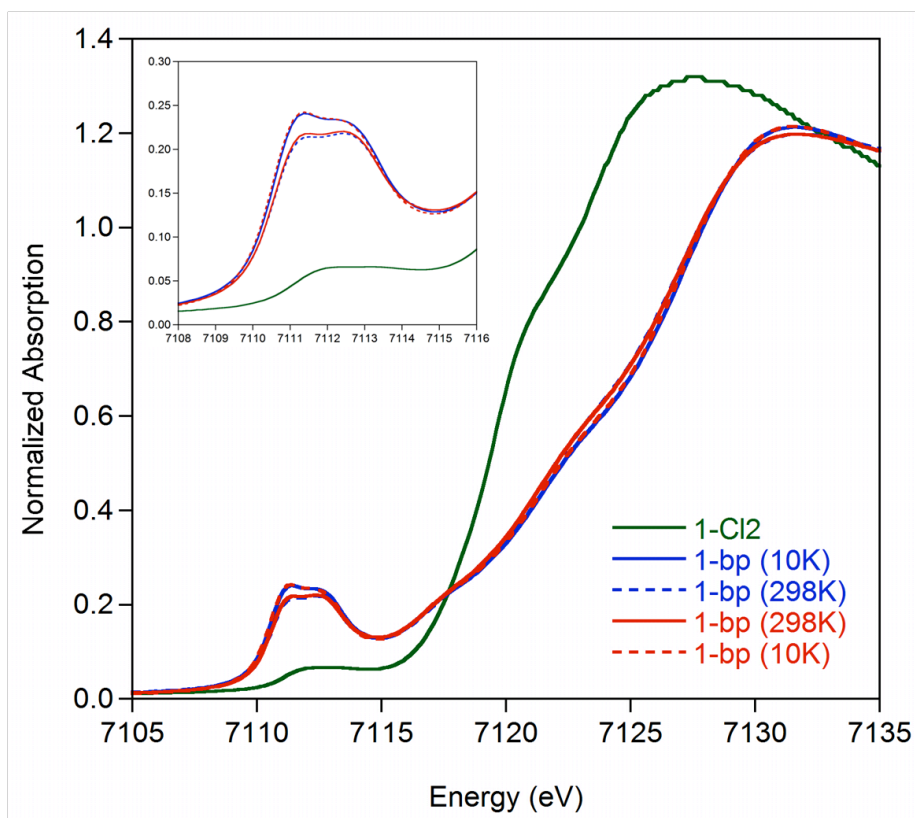


Figure S7. Normalized variable temperature Fe K-edge XAS for (ⁱPrPDI)Fe(biphenyl) (1-bp). Blue lines correspond to the first sample, which was measured at 10 K (solid line), then warmed to 298 K and measured (dotted line). Red lines correspond to the second sample, which was measured at 298 K (solid line), then cooled to 10 K and measured (dotted line). The data for (ⁱPrPDI)FeCl₂ are taken from reference 6. The inset is an expansion of the pre-edge region.

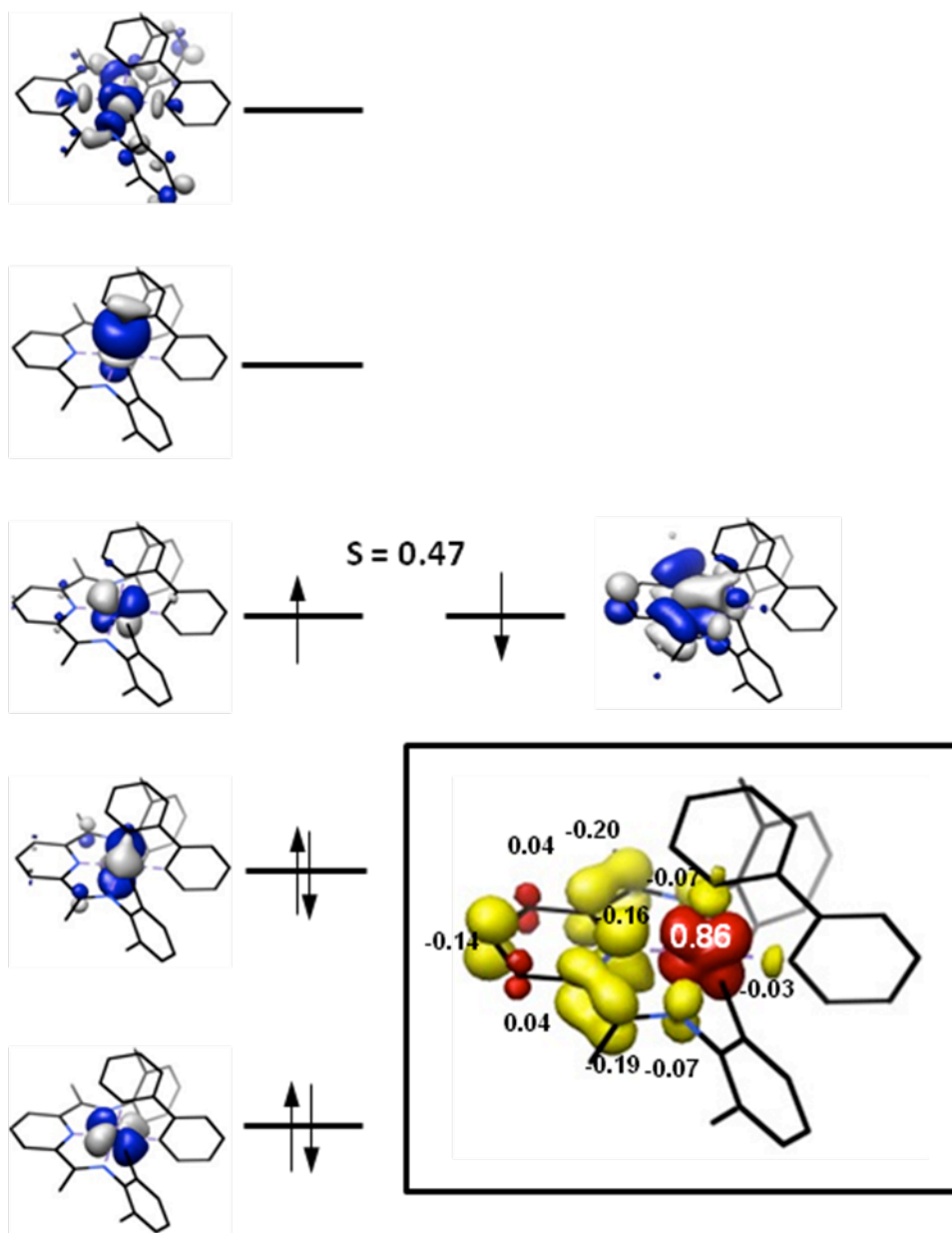


Figure S8. Qualitative localized molecular orbital diagram (left) and spin density plot (inset) obtained from the BS(1,1) solution for $(^{\text{Me}}\text{PDI})\text{Fe}(\text{biphenyl})$. Spin density plot obtained from a Löwdin population analysis of the BS(1,1) solution for $(^{\text{Me}}\text{PDI})\text{Fe}(\text{biphenyl})$ (red = positive spin density, yellow = negative spin density). Total electron densities are Fe = +0.86, PDI = -0.79, biphenyl = -0.08.

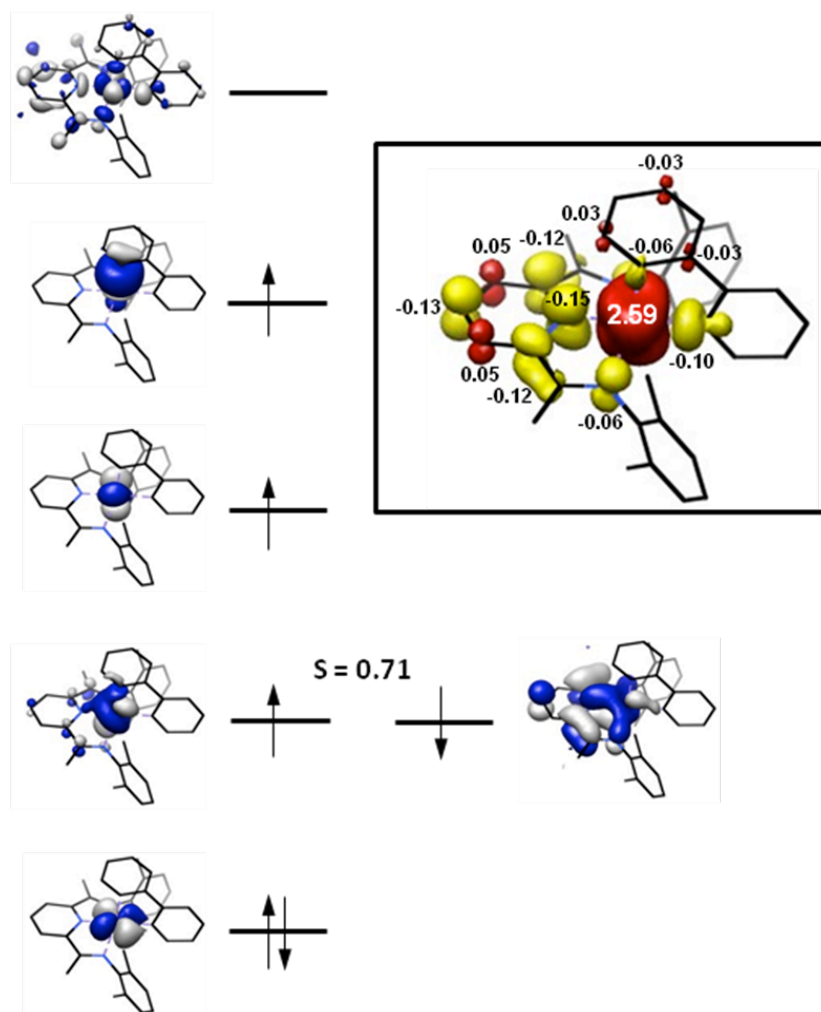


Figure S9. Qualitative localized molecular orbital diagram (left) and spin density plot (inset) obtained from the BS(3,1) solution for $(^{\text{Me}}\text{PDI})\text{Fe}(\text{biphenyl})$. Spin density plot obtained from a Löwdin population analysis of the BS(1,1) solution for $(^{\text{Me}}\text{PDI})\text{Fe}(\text{biphenyl})$ (red = positive spin density, yellow = negative spin density). Total electron densities are Fe = +2.59, PDI = -0.54, biphenyl = -0.06.

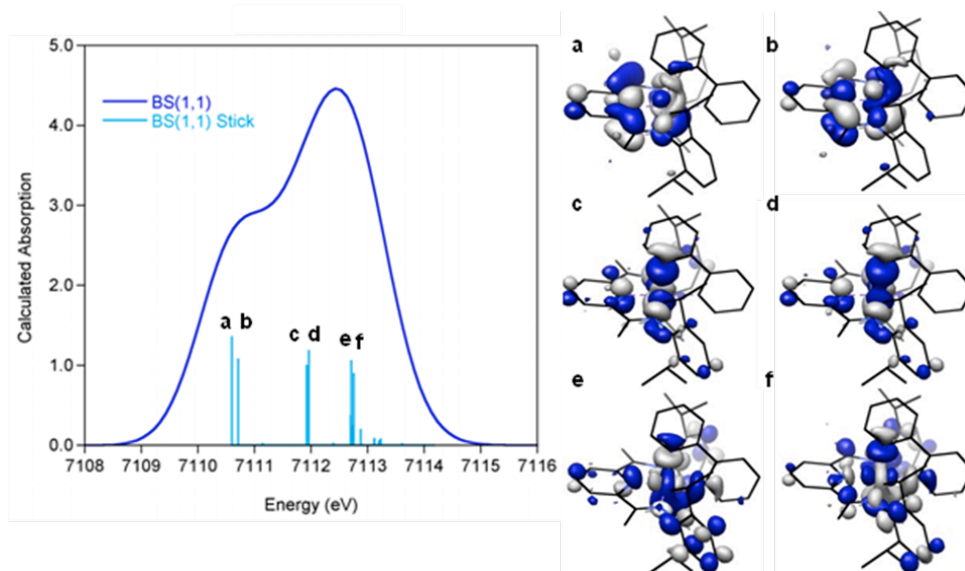


Figure S10. Calculated TDDFT XAS spectrum of ($i\text{PrPDI}$)Fe(biphenyl) BS(1,1) and molecular orbitals corresponding to labeled transitions. A broadening of 1.5 eV and a shift of 181.25 eV have been applied.

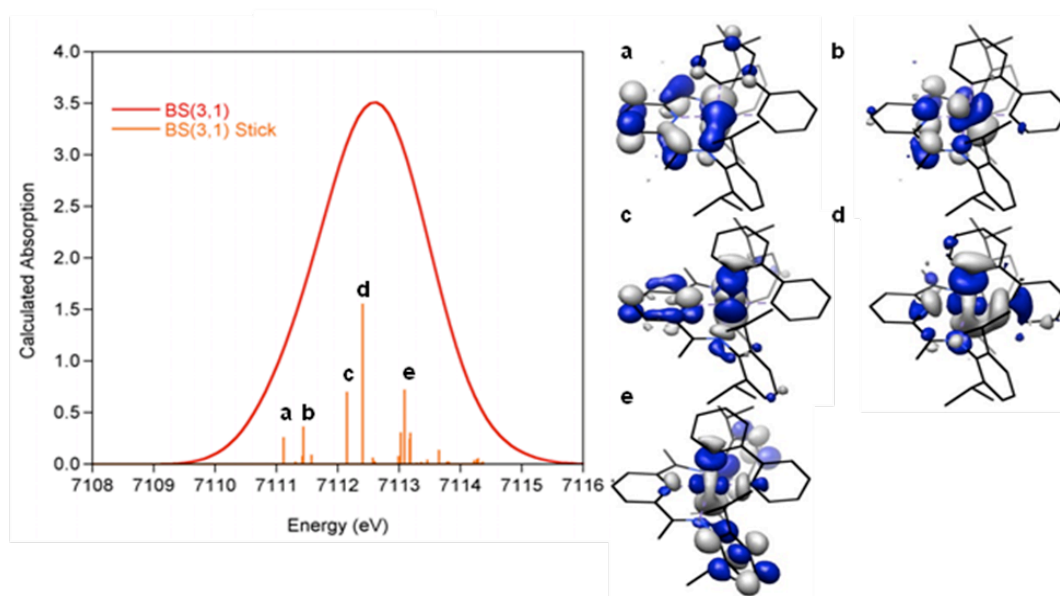


Figure S11. Calculated TDDFT XAS spectrum of ($i\text{PrPDI}$)Fe(biphenyl) BS(3,1) and molecular orbitals corresponding to labeled transitions. A broadening of 1.5 eV and a shift of 181.25 eV have been applied.

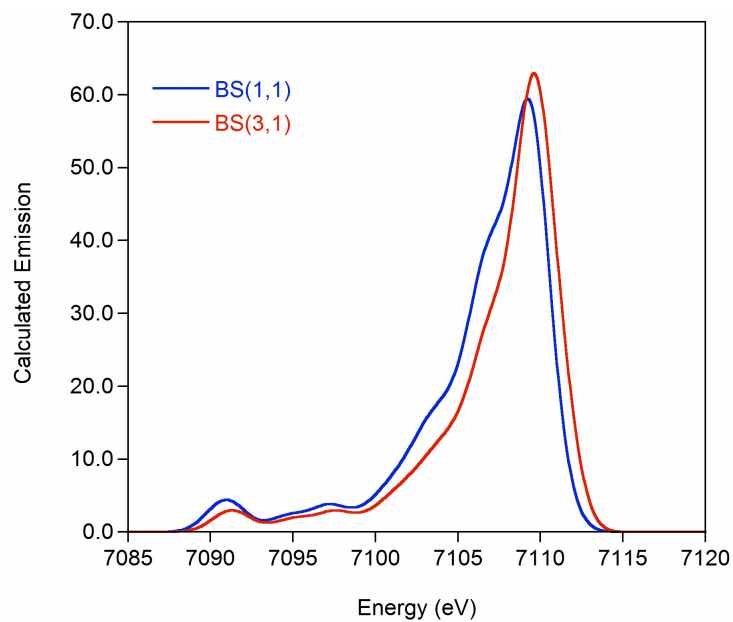
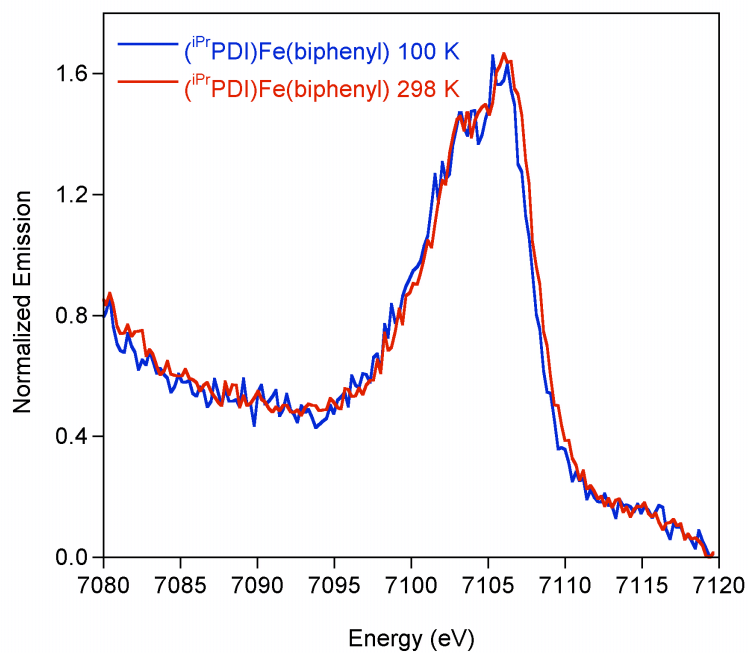


Figure S12. Experimental (top) and calculated (bottom) V2C spectra for $(iPrPDI)Fe(biphenyl)$. A broadening of 2.5 eV and a shift of 182.5 eV have been applied to the computed spectra.¹¹

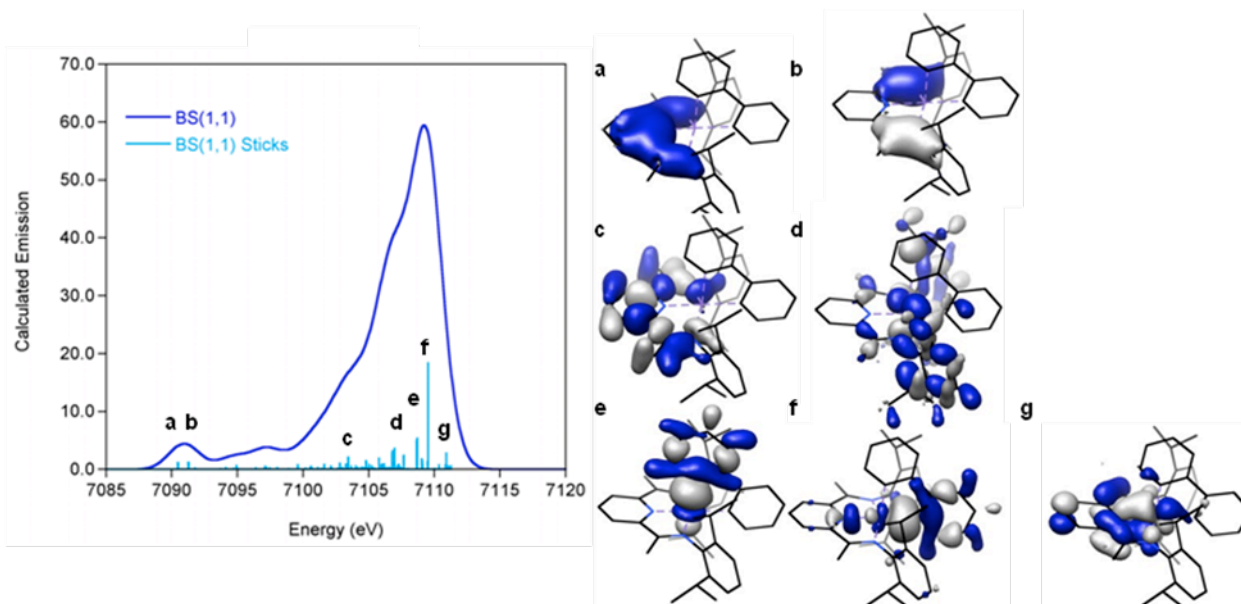


Figure S13. Calculated V2C spectrum of ($i\text{PrPDI}$)Fe(biphenyl) BS(1,1) with molecular orbitals that strongly contribute to the observed transitions. A broadening of 2.5 eV and a shift of 182.5 eV have been applied.

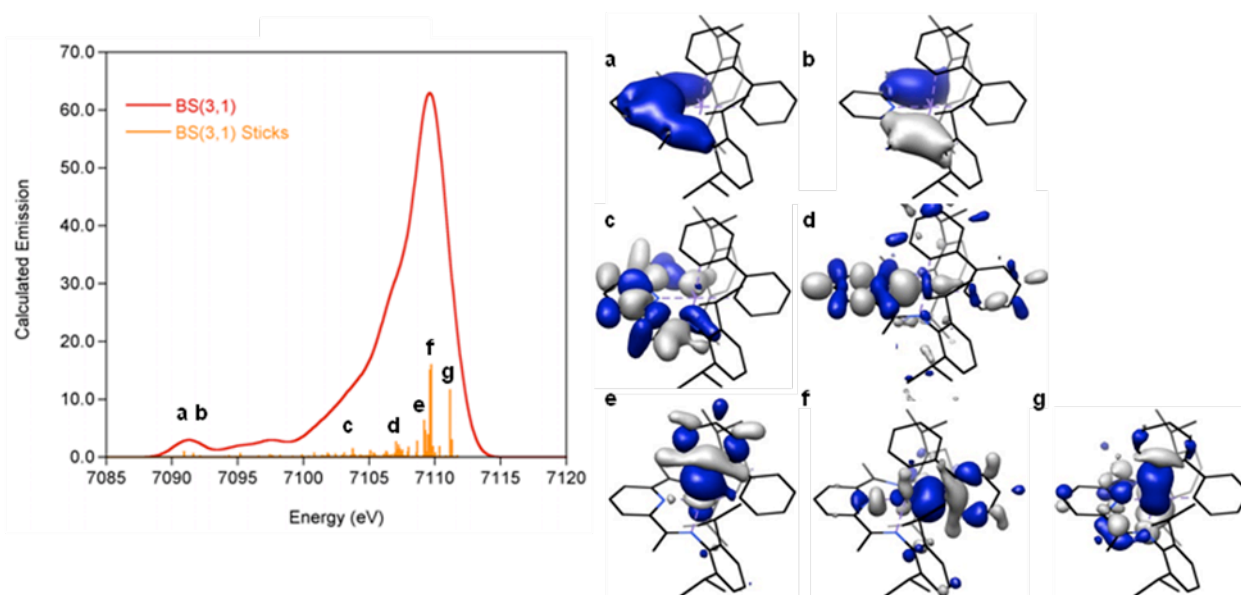


Figure S14. Calculated V2C spectrum of ($i\text{PrPDI}$)Fe(biphenyl) BS(3,1) with molecular orbitals that strongly contribute to the observed transitions. A broadening of 2.5 eV and a shift of 182.5 eV have been applied.

References.

- ¹ Pangborn, A. B.; Giardello, M. A.; Grubbs, R. H.; Rosen, R. K.; Timmers, F. J. *Organometallics* **1996**, *15*, 1518.
- ² Bart, S. C.; Lobkovsky, E.; Chirik, P. J. *J. Am. Chem. Soc.* **2004**, *126*, 13794.
- ³ Russell, S. K.; Darmon, J. M.; Lobkovsky, E.; Chirik, P. J. *Inorg. Chem.* **2010**, *49*, 2782.
- ⁴ Sur, S. K. *J. Magn. Reson.* **1989**, *82*, 169.
- ⁵ Bain, G. A.; Berry, J. F. *J. Chem. Ed.* **2008**, *85*, 532.
- ⁶ Stieber, S. C. E.; Milsmann, C.; Hoyt, J. M.; Turner, Z. R.; Finkelstein, K. D.; Wieghardt, K.; DeBeer, S.; Chirik, P. J. *Inorg. Chem.* **2012**, *55*, 3770.
- ⁷ Neese, F., *Orca: an ab initio, DFT and Semiempirical Electronic Structure Package*, Version 2.8, Revision 2287; Institut für Physikalische und Theoretische Chemie, Universität Bonn: Bonn, Germany, 2010.
- ⁸ Schaub, T.; Radius, U. *Tetrahedron Lett.* **2005**, *46*, 8195.
- ⁹ Kahn, O. *Molecular Magnetism*; VCH: New York, 1993.
- ¹⁰ Sorai, M.; Seki, S. *J. Phys. Chem. Solids* **1974**, *35*, 555.
- ¹¹ Lee, N.; Petrenko, T.; Bergmann, U.; Neese, F.; DeBeer, S. *J. Am. Chem. Soc.* **2010**, *132*, 9715.